



Data-driven learning of nonlocal models: from high-fidelity simulations to constitutive laws

Marta D'Elia^a, Yue Yu^b, Huaiqian You^b, Stewart Silling^d

^aComputational Science and Analysis, Sandia National Laboratories, ^bDepartment of Mathematics, Lehigh University ^cCenter for Computing Research, Sandia National Laboratories



LEHIGH
UNIVERSITY

Abstract. We propose a data-driven approach to learn nonlocal constitutive laws for wave propagation models. In this optimization-based technique the nonlocal kernel function is approximated via Bernstein polynomials and is such that the corresponding nonlocal solution is as close as possible to available high-fidelity data. The optimal nonlocal kernel acts as a homogenized continuum model that accurately reproduces wave motion in a smaller-scale model that can include multiple materials. We apply this technique to wave propagation within a heterogeneous bar, featuring material interfaces at the microscale.

1. Introduction and motivation

Why nonlocal models? Nonlocal models use integral operators acting on a lengthscale δ , known as horizon. This feature allows nonlocal models to capture long-range forces at small scales and multiscale behavior, and to reduce regularity requirements on the solutions, which are allowed to be discontinuous or even singular.

A capability gap. Nonlocal kernels defining nonlocal operators are justified a posteriori and it is not clear how to define such kernels to faithfully describe a physical system.

Main contributions.

- The design of an optimization technique that bridges micro and continuum scales by providing accurate and stable model surrogates for the simulation of wave propagation in heterogeneous materials.
- The illustration of this method via one-dimensional experiments that confirm the applicability of our technique and the improved accuracy compared with state-of-the-art results.
- The demonstration of generalization properties of our algorithm whose associated model surrogates are effective even on problem settings that are substantially different from the ones used for training in terms of loading and time scales.

2. Nonlocal kernel learning

We define the high-fidelity (HF) model that faithfully represents the system: for $\Omega \in \mathbb{R}^d$ and $(x, t) \in \Omega \times [0, T]$

$$\frac{\partial^2 u}{\partial t^2}(x, t) - \mathcal{L}_{\text{HF}}[u](x, t) = f(x, t), \quad (1)$$

augmented with some boundary conditions on $\partial\Omega$ for $u(x, t)$ and initial conditions at $t = 0$ for u and $\partial u/\partial t$.

Assumption 2.1. Solutions to the HF problem may be approximated by solutions to the following nonlocal problem

$$\frac{\partial^2 u}{\partial t^2}(x, t) - \mathcal{L}_K[u](x, t) = f(x, t), \quad (2)$$

for $(x, t) \in \Omega \times [0, T]$, augmented with nonlocal boundary conditions on Ω_δ .

Goal. We seek \mathcal{L}_K as a nonlocal operator of the form

$$\mathcal{L}_K[u](x, t) = \int_{\bar{\Omega}} K(|x-y|) (u(y, t) - u(x, t)) dy, \quad (3)$$

where $\bar{\Omega} = \Omega \cup \Omega_\delta$ and K is a radial, sign-changing, kernel function, compactly supported on $B_\delta(x)$, such that the corresponding problem (2) is a good approximation of (1).

The Algorithm. We assume that we are given N pairs of forcing terms and corresponding solutions to (1) for $x \in \Omega$ and $t \in (0, T_{\text{tr}}]$: $\mathcal{D}_{\text{tr}} = \{(u_k(x, t), f_k(x, t))\}_{k=1}^N$. We represent K as a linear combination of Bernstein basis polynomials [1]:

$$K\left(\frac{|y|}{\delta}\right) = \sum_{m=0}^M \frac{C_m}{\delta^{d+2}} B_{m,M}\left(\frac{|y|}{\delta}\right), \quad B_{m,M}(x) = \binom{M}{m} x^m (1-x)^{M-m} \quad (4)$$

for $0 \leq x \leq 1$ and $C_m \in \mathbb{R}$. By construction this kernel guarantees that (2) is **well-posed** [2].

We approximate solutions to (2), for $f = f_k$ and the kernel function K by \bar{u}_k using a central-differencing scheme in time with time step dt , i.e.

$$\bar{u}_k^{n+1}(x_i) = 2\bar{u}_k^n(x_i) - \bar{u}_k^{n-1}(x_i) + dt^2 (\mathcal{L}_{K,h}[\bar{u}_k^n](x_i) + f_k(x_i, t^n)), \quad (5)$$

where $\bar{u}_k^{n+1}(x_i)$ represents the k -th approximate solution at time step t^{n+1} and at discretization point x_i , and $\mathcal{L}_{K,h}$ is an approximation of \mathcal{L}_K by Riemann sum with uniform grid spacing h .

The optimal parameters are obtained by solving

$$\min_{C_m} \frac{T_{\text{tr}}}{dt^3 N} \sum_{k=1}^N \sum_{n=1}^{T_{\text{tr}}/dt} \|\bar{u}_k^{n+1} - u_k(t^{n+1})\|_{\ell^2}^2 + \mathcal{R}(\{C_m\}), \quad (6)$$

$$\text{s.t. } \bar{u}_k \text{ satisfies (5) and} \quad (7)$$

$$K \text{ satisfies physics-based constraints.} \quad (8)$$

Here, $\mathcal{R}(\cdot)$ is a regularization term on the coefficients that improves the conditioning of the optimization problem, and (8) depends on the physics of the problem.

3. Application to dispersion in heterogeneous materials

We consider the propagation of waves in a one-dimensional heterogeneous bar, like the one reported in Figure 1, with an *ordered* microstructure. We learn a nonlocal model able to reproduce wave propagation on distances that are much larger than the size of the microstructure without resolving the microscales.

The high-fidelity model we rely on is the classical wave equation and the corresponding high-fidelity data are obtained with a Direct Numerical Simulation (DNS) solver.

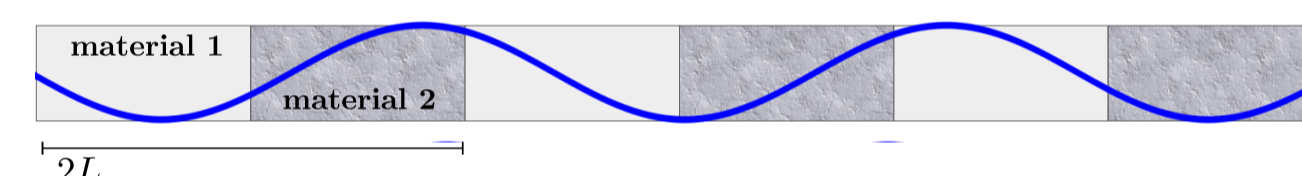


Figure 1: One-dimensional bar with ordered microstructure of period $2L$. Materials 1 and 2 have the same density and Young modulus E_1 and E_2 .

High-fidelity data. We consider four types of data and use the first two for training and the last two for validation of our algorithm. In all our experiments we set $L = 0.2$, $E_1 = 1$, $E_2 = 0.25$, $\rho = 1$, and the symmetric domain $\Omega = (-b, b)$.

1) Oscillating source. We set $b = 50$, $\dot{u}(x, 0) = u(x, 0) = 0$,

$$f(x, t) = e^{-\frac{2x}{5kL}} e^{-\left(\frac{t-t_0}{t_p}\right)^2} \cos^2\left(\frac{2\pi x}{kL}\right), \quad k = 1, 2, \dots, 20, \quad t_0 = t_p = 0.8.$$

2) Plane wave. For $b = 50$, $f(x, t) = 0$ and $u(x, 0) = 0$, we prescribe $\dot{u}(-b, t) = \sin(\omega t)$ for $\omega = 0.35, 0.7, \dots, 3.85$.

3) Wave packet. For $b = 133.3$, $f(x, t) = 0$ and $u(x, 0) = 0$, we prescribe $\dot{u}(-b, t) = \sin(\omega t) \exp(-(t/5 - 3)^2)$ for $\omega = 2, 3.9, 5$.

4) Impact. For $b = 266.6$, $f(x, t) = 0$ and $u(x, 0) = 0$, we prescribe $\dot{u}(x, 0) = 1$ for all $x \in [-b, -b + 1.6]$ and $v = 0$ outside of this interval. This initial condition represents an impactor hitting the bar at $t = 0$, generating a velocity pulse that propagates into the bar.

Training procedure. For the optimization problem (6) we choose a Tikhonov regularization of the form $\mathcal{R}(\{C_m\}) = \frac{\epsilon}{M+1} \sum_{m=0}^M C_m^2$, where the regularization weight ϵ is chosen empirically. The physics-based constraints in (8) are defined as follows and are used to explicitly prescribe values of C_{M-1} and C_M :

$$\sum_{m=0}^M C_m \int_0^\delta \frac{y^2}{\delta^3} B_{m,M}\left(\frac{|y|}{\delta}\right) dy = \rho c_0^2, \quad \sum_{m=0}^M C_m \int_0^\delta \frac{y^4}{\delta^3} B_{m,M}\left(\frac{|y|}{\delta}\right) dy = -4\rho c_0^3 R, \quad (9)$$

where ρ is the density of the bar and c_0 is the effective wave speed for infinitely long wavelengths. For $\rho = 1$, it is given by $c_0 = (2/(1/E_1 + 1/E_2))^{1/2}$. $2R$ is the second derivative of the wave group velocity with respect to the frequency ω evaluated at $\omega = 0$.

Training is performed with DNS data of type 1) and 2). Parameters for the nonlocal solver and the optimization algorithm are set to $h = 0.05$, $dt = 0.02$, $T_{\text{tr}} = 2$, $\delta = 1.2$, $M = 24$ and $\epsilon = 0.01$. The optimization problem (6) is solved with L-BFGS.

The optimal kernel, K_{opt} , is reported in Figure 2 (left). We also compute the corresponding dispersion $\omega(k)$ and group velocity $v_g(\omega) = d\omega/dk$. The dispersion curve is reported in Figure 2 (center); the group velocity is reported in Figure 2 (right). We also display the group velocity associated with an alternative, constant kernel, K_{const} , obtained for the same material by the method described in [3].

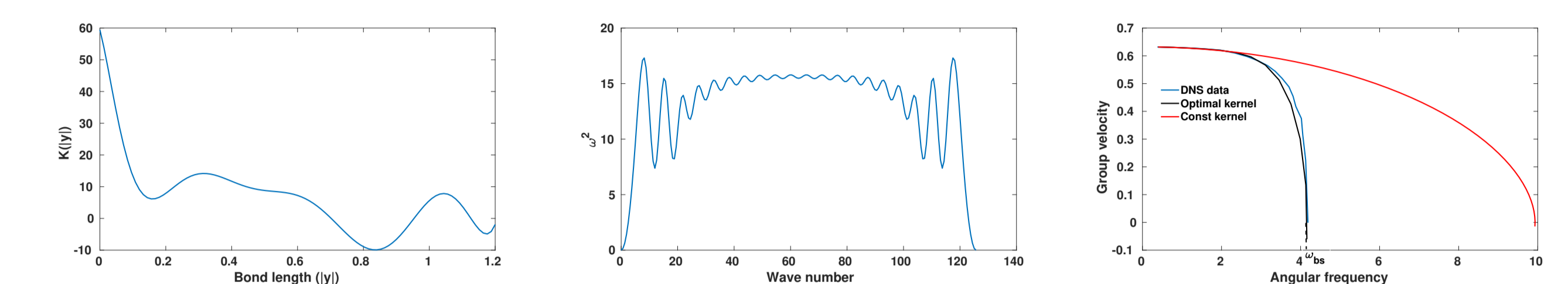


Figure 2: Left: optimal kernel as a function of distance. Center: dispersion curve; its positivity implies the stability of the material model. Right: group velocity for K_{opt} , K_{const} and DNS; these profiles show the improved accuracy of K_{opt} that not only matches the behavior for low values of ω , but also catches the behavior at $\omega = \omega_{\text{bs}}$, where a band stop occurs.

4. Validation

We test the performance of the optimal kernel K_{opt} on data sets of type 3) and 4): the problem setting considered for validation has different model parameters, including the domain, than the one used for training. These tests illustrate the excellent **generalization properties** of our algorithm.

Wave packet. We consider solutions corresponding to three values of ω : $\omega_1 = 2 < \omega_{\text{bs}}$, $\omega_2 = 3.9 \approx \omega_{\text{bs}}$ and $\omega_3 = 5 > \omega_{\text{bs}}$. Note that the latter value is beyond the band stop and, as such, corresponds to a zero group velocity, i.e. the wave does not travel in time. In Figure 3, from left to right, we report the velocity corresponding to the computed displacement.

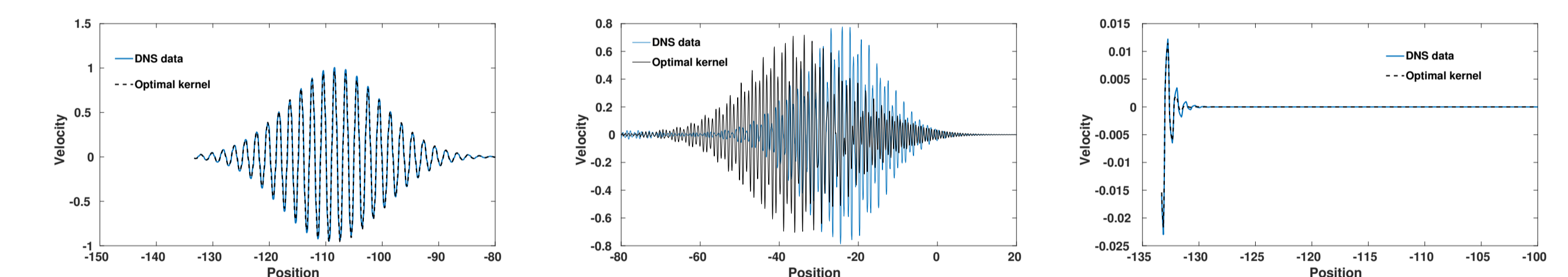


Figure 3: From left to right, velocity at time $t = 100$, $t = 320$, and $t = 100$ for ω_1 , ω_2 , and ω_3 respectively for both K_{opt} and DNS. Our kernel can accurately reproduce solutions of type 3) at times larger than T_{tr} and for all values of ω , even larger than ω_{bs} thanks to the accurate agreement with the group velocity.

Impact. In Figure 4 we report the velocity profile at different time steps in correspondence of K_{opt} and DNS data, displayed for comparison.

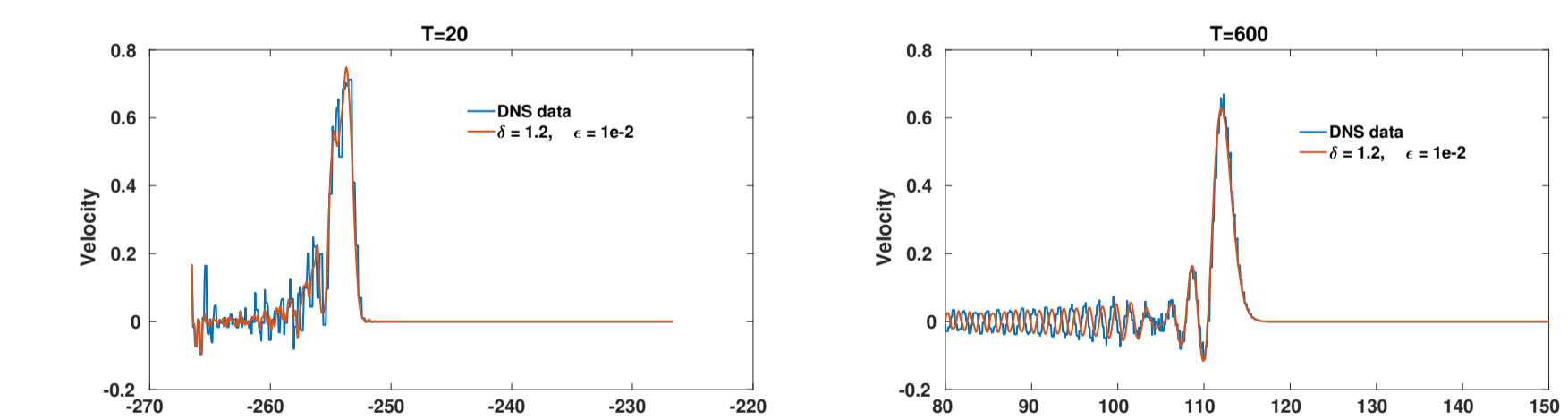


Figure 4: Velocity for the impact problem at time $T = 20$ (left) and $T = 600$. Our optimal kernel can accurately predict the short- and long-time wave propagation.

5. Selected References

1. You, H.; Yu, Y.; Trask, N.; Gulian, M.; and D'Elia, M. 2020. Data-driven learning of robust nonlocal physics from high-fidelity synthetic data. ArXiv:2005.1007
2. Du, Q.; Tao, Y.; and Tian, X. 2018. A peridynamic model of fracture mechanics with bond-breaking. Journal of Elasticity 132(2): 197-218.
3. Silling, S. 2020. Propagation of a Stress Pulse in a Heterogeneous Elastic Bar. Sandia Report SAND2020-8197, Sandia National Laboratories

This work supported is by the Sandia National Laboratories (SNL) Laboratory-directed Research and Development program and by the U.S. Department of Energy, Office of ASCR under the Collaboratory on Mathematics and Physics-Informed Learning Machines for Multiscale and Multiphysics Problems project. SNL is a multi-mission laboratory managed and operated by National Technology and Engineering Solutions of Sandia, LLC, a wholly owned subsidiary of Honeywell International, Inc., for the U.S. Department of Energy's National Nuclear Security Administration under contract DE-NA-0003525.